J|A|C|S
ARTICLES
Published on Web 02/02/2006

# Demonstration of the Ring Conformation in Polyproline by the Raman Optical Activity

Josef Kapitán,[†,‡] Vladimír Baumruk,[†,‡] and Petr Bouř*[,†]

*Contribution from the Institute of Organic Chemistry and Biochemistry, Academy of Sciences, Flemingovo nám 2, 16610, and Charles University, Faculty of Mathematics and Physics, Institute of Physics, Ke Karlovu 5, 12116, Prague, Czech Republic*

Received October 27, 2005; E-mail: bour@uochb.cas.cz

***Abstract:*** Raman and Raman optical activity (ROA) spectra of poly-L-proline were recorded in a wide frequency range and analyzed with respect to the proline side chain conformation. The analysis was based on comparison to ab initio simulations of spectral band positions and intensities. The presence of two conformer states of the five-member ring was found, approximately equally populated in the polypeptide. Additionally, Raman and ROA spectral shapes indicated that the peptide adopts the polyproline II helical conformation, in both aqueous and TFE solutions. The helix, however, is perturbed by fluctuations, which affects the vibrational coupling among amino acid residues and broadens the ROA bands. Contributions of the side and main peptide chains to the polyproline ROA intensities have comparable magnitudes. Thus understanding of the origins of both signals is important for determination of the peptide structure by ROA.

## Introduction

While peptide and protein conformational studies are important for elucidation of their biological functions, stabilities, and interactions in enzyme−substrate complexes, the role of detailed amino acid composition in these interactions involving solvation, flexibility, structure, and conformation of peptide side chains is rather unexplored. The Raman optical activity (ROA) spectroscopy is a new promising technique that can provide relatively easy some of the structural information.[1−4] The technique measures the difference in scattering of the right- and left-circularly polarized light.[5] Similarly as the vibrational circular dichroism (VCD)[6] the ROA spectra reflect the conformation of the main peptide chain. Additionally, however, the peptide side chains, often hydrophobic hydrocarbon structures, provide strong Raman and ROA signals within almost the entire frequency region due to the polarizability changes during their vibrational motion.[5,7] Interactions determining the ROA signal are also believed to be more local than for VCD,[7−10] which enables studying finer structural features and, in combination with isotopic labeling,[11] may potentially bring higher spatial resolution. Despite this potential, rather few ROA studies dedicated to the peptide side chains behavior are known.[1] On the other hand, correlation of the peptide main chain secondary structure and ROA signal was explored on a number of model systems, globular proteins, and even viruses.[2,3,12] One of the obstacles in analyzing the side chain signal is an inadequacy of the usual static modeling neglecting the chain motions and conformational equilibria. Moreover, ab initio simulations of ROA intensities necessary for correct spectra interpretation are very demanding on computational power. Principal obstacle consists of evaluation of the optical activity tensor derivatives, essentially a third-order energy derivative that has to be calculated by a tedious numerical differentiation.[13]

However, as shown below, ring conformations in the poly-L-proline chain are clearly reflected by the ROA spectra, and the presence of two conformers (**A**, **B**, Figure 1) can be manifested. The polyproline left-handed helix ("polyproline II", PPII) itself is thought to be a good model for so-called random peptide conformation.[14,15] In fact, there are several ROA studies of nonproline peptides adopting this conformation,[16,17] but none with the polyproline itself. Separation of the main- and side-chain signal thus appears important for further development of

[†] Academy of Sciences.
[‡] Charles University.

(1) Blanch, E. W.; Hecht, L.; Day, L. A.; Pederson, D. M.; Barron, L. D. *J. Am. Chem. Soc.* **2001**, *123* (20), 4863−4864.
(2) Barron, L. D.; Blanch, E. W.; McColl, I. H.; Syme, C. D.; Hecht, L.; Nielsen, K. *Spectroscopy (Amsterdam, Neth.)* **2003**, *17* (2−3), 101−126.
(3) Blanch, E. W.; Hecht, L.; Barron, L. D. *Methods* **2003**, *29* (2), 196−209.
(4) Barron, L. D.; Hecht, L.; Blanch, E. W.; Bell, A. F. *Prog. Biophys. Mol. Biol.* **2000**, *73*, 1−49.
(5) Barron, L. D. *Molecular Light Scattering and Optical Activity*; Cambridge University Press: Cambridge, 2004.
(6) Keiderling, T. A. Circular Dichroism. In *Circular dichroism: principles and applications*, 2nd ed.; Berova, N., Nakanishi, K., Woody, R. W., Eds.; Wiley: New York, 2000; pp 621−666.
(7) Nafie, L. A. *Annu. Rev. Phys. Chem.* **1997**, *48*, 357−386.
(8) Polavarapu, P. L. *Vibrational spectra: principles and applications with emphasis on optical activity*. Elsevier: Amsterdam, 1998; Vol. 85.
(9) Tam, C. N.; Bouř, P.; Keiderling, T. A. *J. Am. Chem. Soc.* **1997**, *119* (30), 7061−7064.
(10) Qu, X. H.; Lee, E. A.; Yu, G. S.; Freedman, T. B.; Nafie, L. A. *Appl. Spectrosc.* **1996**, *50* (5), 649−657.
(11) Silva, R. A. G. D.; Kubelka, J.; Decatur, S. M.; Bour, P.; Keiderling, T. A. *Proc. Natl. Acad. Sci. U.S.A.* **2000**, *97* (15), 8318−8323.
(12) Blanch, E. W.; Morozova-Roche, L. A.; Hecht, L.; Noppe, W.; Barron, L. D. *Biopolymers* **2000**, *57* (4), 235−248.
(13) Ruud, K.; Helgaker, T.; Bouř, P. *J. Phys. Chem. A* **2002**, *106* (32), 7448−7455.
(14) Dukor, R. K.; Keiderling, T. A. *Biopolymers* **1991**, *31*, 1747−1761.
(15) Dukor, R. K.; Keiderling, T. A. *Biospectroscopy* **1996**, *2*, 83−100.
(16) McColl, I. H.; Blanch, E. W.; Hecht, L.; Kallenbach, N. R.; Barron, L. D. *J. Am. Chem. Soc.* **2004**, *126* (16), 5076−5077.
(17) Blanch, E. W.; Gill, A. C.; Rhie, A. G. O.; Hope, J.; Hecht, L.; Nielsen, K.; Barron, L. D. *J. Mol. Biol.* **2004**, *343* (2), 467−476.


**10.1021/ja057337r CCC: $33.50** 

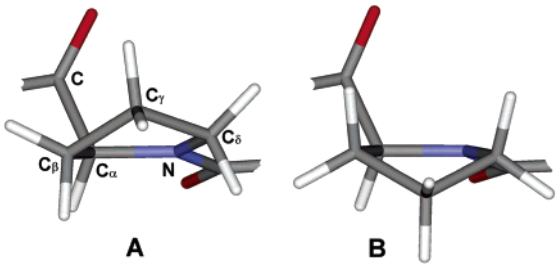


***Figure 1.*** Two conformations of the proline ring in the polyproline chain.

the ROA technique. Detailed analysis of the polyproline signal was enhanced by the latest upgrade of our spectrometer.[18] ROA spectra with a high signal-to-noise ratio could be obtained within an unusually broad frequency region of about 70−2300 $cm^{-1}$. Also, the molecular property tensor transfer technique[19] enabled us to derive spectral responses of long peptide segments from reasonably accurate quantum computations on smaller tripeptide fragments.

## Methods

**Experiment.** The backscattered Raman and incident circular polarization (ICP) ROA spectra were recorded on our spectrometer described elsewhere.[20,21] Recently, the apparatus was upgraded and is currently based on a fast stigmatic spectrograph HoloSpec HS-f/1.4 (Kaiser Optical Systems) equipped with a holographic transmission grating and a back-illuminated CCD detection system (Roper Scientific, 1340 × 100 pixels). The poly-L-proline was purchased from Sigma (P-2129, MW 10.000−30.000) and used without further purification. Nearly saturated solutions of the peptide in doubly distilled deionized water (∼10 mg/mL) and in 2,2,2-trifluoroethanol (∼42 mg/mL, TFE purchased from Aldrich; Cat. No. 32,674-7) were prepared and filtered through a 0.22 $\mu$m Millipore filter into a standard 5 × 5 $mm^2$ quartz microfluorescence cell (Hellma). To minimize and stabilize spectral background, residual fluorescence coming from traces of impurities in the peptide was quenched by leaving the sample to equilibrate in the laser beam for several hours before the acquisition. The experimental conditions were as follows: room temperature (∼293 K), 514.5 nm excitation wavelength, laser power at the sample ∼570 mW, spectral resolution of 6.5 $cm^{-1}$, total acquisition times of 44 and 28.5 h for aqueous and TFE solutions, respectively. The solvent signal was subtracted from Raman spectra, and then a baseline correction was made. A raw ROA spectrum was Fourier filtered to suppress quasi-periodic high spatial-frequency signal in the low wavenumber region, corrected for an artifact spurious signal from solvent and cell walls and finally subjected to a minor baseline correction when necessary.[18,22]

**Calculations.** For model tripeptide fragments HCO−(L-Pro)$_3$−$NH_2$ harmonic force fields and ROA intensity tensors were calculated by the Gaussian program.[23] The standard polyproline II secondary structure ($\varphi = -78°$, $\psi = 149°$, $\omega = 180°$)[24] was used as a starting geometry, and all eight possible combinations of the five-membered proline ring were investigated (AAA, AAB, ABA, BAA, ABB, BAB, BBA, and BBB). These structures were subjected to a full optimization in order to determine conformer energetics, as well as to a restricted normal-mode optimization,[25] so that only vibrations important for the experimental spectrum could be relaxed with a minimal change of the polyproline II main chain conformation. Our QGRAD program[25−27] was used for the normal mode optimization with modes fixed within −100...200 $cm^{-1}$. The optimizations and the force field computations were performed at the B3LYP/COSMO[28]/6-31G** level, while the Raman and ROA polarizability tensors were obtained at the HF/6-31G level. A simplified polarization model[21] exploring dependence of the magnetic and quadrupole polarizabilities on the coordinate system[29] was alternatively used for some trial ROA intensity simulations. For this latter approach only the "ordinary" electric dipole polarizability available on a high B3LYP/COSMO/6-31G** level was needed. Force field and polarizability tensors of longer poly-L-proline segments were obtained from the tripeptide fragments by transfer in Cartesian coordinates.[19] During the transfer the source tripeptides in proper conformations were propagated along the polyproline chain as indicated in Figure 2. Thus the spectra could be simulated for proline oligomers containing 3, 5, 10, and 20 proline residues.

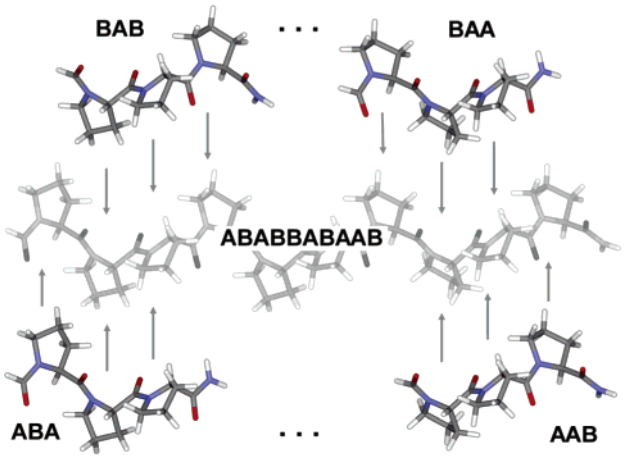


***Figure 2.*** Schematic representation of the tensor transfer. Atomic property tensors (second energy derivatives (Hessian), and the electric dipole−electric dipole, electric dipole−electric quadrupole, and electric dipole−magnetic dipole polarizability derivatives) in the tripeptides were obtained ab initio and transferred by propagation of these smaller fragments in suitable conformation along the longer polypeptide chain.

The Raman and ROA spectra were generated within the harmonic approximation using the usual procedure.[21,30,31] With programs written in house the tensor transfer (Figure 2) could be done for arbitrary conformer sequences in proline oligomers. For each conformer population (e.g., 50% of **A**) such geometries were obtained by a random generator, and for each spectra frequencies and intensities were calculated via the transfer. To obtain representative statistical ensembles of 3-, 5-, 10-, and 20-mers, 8, 32, 1024, and 50 sequences of **A** and **B** were averaged, respectively. (The inclusion of all the 1024 permutations for the 10-mer had little practical effect; a fraction of the total number provided spectra satisfactory enough.) The calculated spectra were divided by molecular weight so that the simulated relative intensities for peptides of different lengths had a physical meaning. Note that absolute intensities cannot be obtained by experiment.

(18) Kapitán, J.; Baumruk, V.; Gut, V.; Hlaváček, J.; Dlouhá, H.; Urbanová, M.; Wunsch, E.; Maloň, P. *Collect. Czech. Chem. Commun.* **2005**, *70* (4), 403−409.
(19) Bouř, P.; Sopková, J.; Bednárová, L.; Maloň, P.; Keiderling, T. A. *J. Comput. Chem.* **1997**, *18*, 646−659.
(20) Hanzliková, J.; Praus, P.; Baumruk, V. *J. Mol. Struct.* **1999**, *481*, 431−435.
(21) Bouř, P.; Baumruk, V.; Hanzliková, J. *Collect. Czech. Chem. Commun.* **1997**, *62* (9), 1384−1395.
(22) Kapitán, J.; Baumruk, V.; Hulačová, H.; Maloň, P. *Vib. Spectrosc.*, submitted.
(23) Frisch, M. J. at al. *Gaussian 03*, revision C.02; Gaussian, Inc.: Wallingford, CT, 2004.
(24) Creighton, T. E. *Proteins*; W. E. Freeman and Co.: New York, 1984.
(25) Bouř, P.; Keiderling, T. A. *J. Chem. Phys.* **2002**, *117*, 4126−4132.
(26) Bouř, P. *Chem. Phys. Lett.* **2002**, *365*, 82−88.
(27) Bouř, P. *Collect. Czech. Chem. Commun.* **2005**, *70*, 1315−1340.
(28) Klamt, A. *J. Phys. Chem.* **1995**, *99*, 2224−2235.
(29) Bouř, P. *Chem. Phys. Lett.* **1998**, *288* (2−4), 363−370.
(30) Nafie, L. A.; Che, D. Theory and Measurement of Raman Optical Activity. In *Modern Nonlinear Optics, Part 3*; Evans, M., Kielich, S., Eds.; Wiley: New York, 1994; Vol. 85, pp 105−149.
(31) Hug, W. *Chimia* **1994**, *48* (9), 386−390.

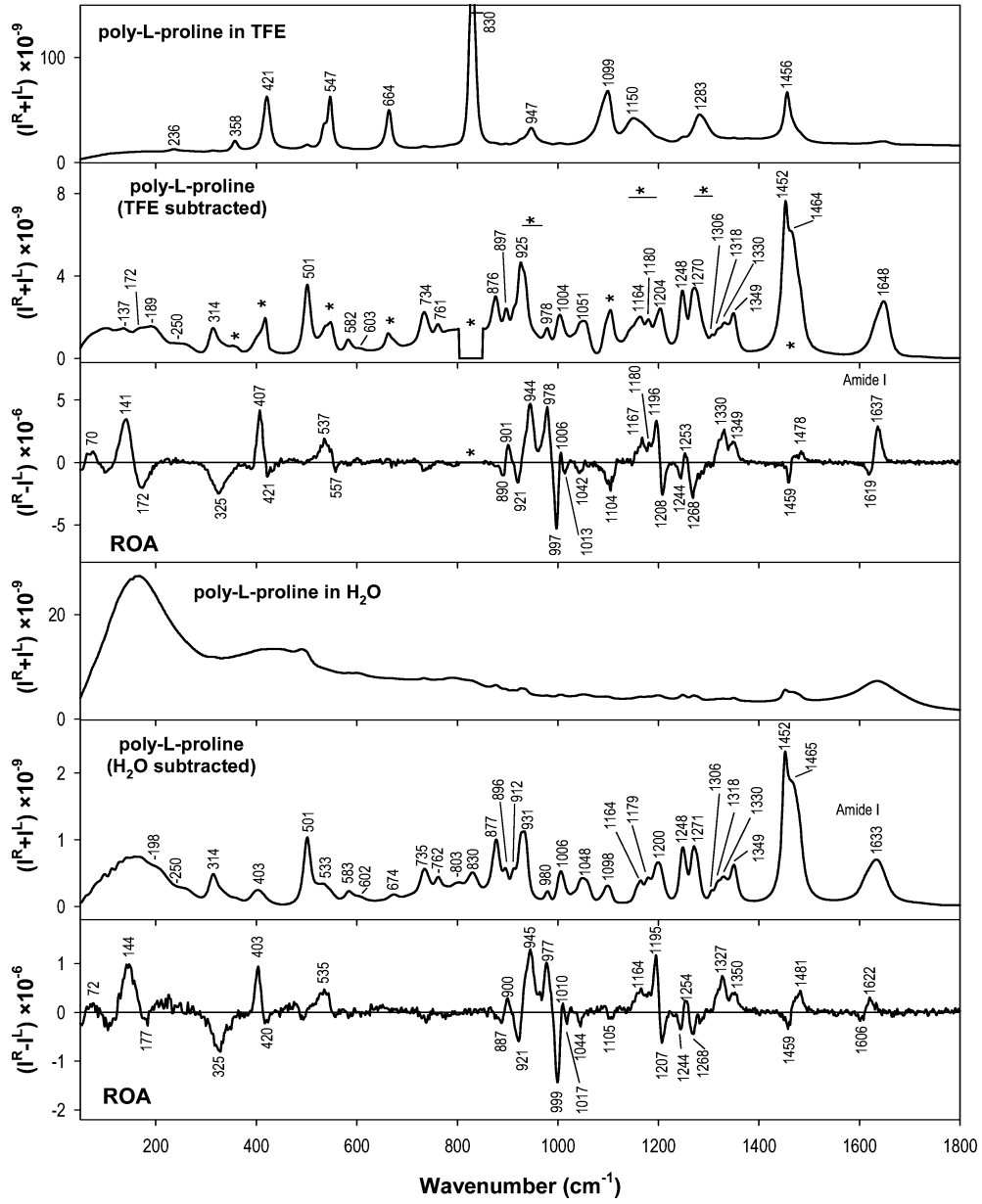


***Figure 3.*** Poly-L-proline Raman ($I^R + I^L$) and ROA ($I^R - I^L$) experimental spectra, including the raw Raman traces, for the TFE and $H_2O$ solvents. For TFE, regions of strong solvent interference are marked by an asterisk (*). The intensity scale expresses the total number of detected counts.

## Results and Discussion

**Proline Geometry.** As can be estimated from relative conformer energies for all possible tripeptide ring sequences listed in Table 1, the proline ring flipping (Figure 1) does not significantly change molecular energy. The energies are comparable with the temperature Boltzmann quantum (~0.6 kcal/mol) and lie below the expected accuracy of the ab initio method. In this context, the zero-point vibrational energy (ZPE) corrections appear rather negligible. The pseudorotation concept developed by Cremer and Pople was used for the description of the geometry of the proline ring.[32] Unlike previous approaches, it does not introduce artificial approximations. In accord with other studies[33] we did not find significant differences between this approach and modified definitions of the coordinates sometimes used for saccharides. The predicted pucker phase angles[32] lie between 15° and 24° for **A** and 178° and 194° for **B**, while puckering amplitudes[32] are close to 0.4 Å for both cases. Strictly speaking, the phase changes in individual rings are not independent. For example, the relative energy of

***Table 1.*** Relative Energies ($E$, kcal/mol) and Proline Ring Phases ($\chi_{1-3}$, deg)[32] for Fully Optimized Tripeptide HCO−(L-Pro)$_3$−$NH_2$ Conformers Calculated at the B3LYP/COSMO/ 6-31G** Level

| conformer | $E$ | $E$ + ZPE | $\chi_1$ | $\chi_2$ | $\chi_3$ |
|---|---|---|---|---|---|
| **AAA** | 0 | 0.1 | 17 | 24 | 20 |
| **AAB** | 0.6 | 0.7 | 18 | 16 | 193 |
| **ABA** | 0.6 | 0.6 | 11 | 192 | 19 |
| **ABB** | 0.8 | 1.1 | 10 | 194 | 194 |
| **BAA** | 0.1 | 0.2 | 178 | 22 | 21 |
| **BAB** | 0.6 | 0.7 | 181 | 15 | 192 |
| **BBA** | 0.5 | 0.6 | 181 | 191 | 20 |
| **BBB** | 0.4 | 0.7 | 181 | 194 | 194 |
| **A**[a] | 0 | | 18 | | |
| **B**[a] | 0.4 | | 168 | | |

[a] Monomer HCO−Pro−H.

(32) Cremer, D.; Pople, J. A. *J. Am. Chem. Soc.* **1975**, *97* (6), 1354−1358.
(33) Harvey, S. C.; Prabhakaran, M. *J. Am. Chem. Soc.* **1986**, *108*, 6128−6136.

**BBB**, naively generated from **AAA** via three **A**→**B** transitions, is not 3 times bigger than that for **AAB**. In fact, it is smaller! This cooperation might suggest that certain sequences (**AAA**, **BAA**) occur more frequently than others (e.g., **ABB**), but the energy differences are rather small and present methodology cannot reveal such nuances. Thus we based the modeling on a random sequence distribution and biased the total **A** and **B** populations only. The secondary structure of the optimized tripeptides did not significantly deviate from the initial polyproline II geometry (Tables 1s, 2s in the Supporting Information).

**Experimental Spectra.** In Figure 3 the spectra covering most of the frequency region available by our spectrometer are plotted. Several features typical for the Raman and ROA spectroscopy of biopolymers can be documented. Both the TFE and aqueous solvents contribute significantly to the Raman signal of the sample, while the solute itself (in a rather high concentration!) makes less than 10% of the total intensity. By careful baseline subtraction, however, the polyproline spectrum can be reliably recovered. Unfortunately, numerous sharp TFE solvent bands interfere with the solute signal and obscure some polyproline Raman bands (marked by the asterisk * in Figure 3).

The ROA baseline signal of the solvent was stable during the measurement, making at most 10% of the sample signal, and could be reliably subtracted. However, the most intense TFE Raman peak at 830 $cm^{-1}$ prevents us from obtaining reliable ROA in the vicinity. Fortunately no solute ROA bands are present in this region, as could be verified for the aqueous sample. Also, we could indirectly exclude artifact ROA signals on the basis of measurement of similar compounds (L- and D-proline) for which both optical isomers were available and by time checks of stability of spectrometer parameters. The broad Raman signal of water below ~200 $cm^{-1}$ interferes with the solute response in this region, although instrumental limits allow measurement down to ~70 $cm^{-1}$.

The polyproline band positions and intensities are remarkably similar for the two solvents, except those of the amide I peak. This mode (C═O stretching, 1648 $cm^{-1}$ in TFE, 1633 $cm^{-1}$ in $H_2O$) is most influenced by formation of hydrogen bonds and solvent polarity. The ROA sign patterns within 900−1010 $cm^{-1}$ (+ − + + −) and 1164−1207 $cm^{-1}$ (+ + −) seem to be characteristic for polyproline in the PPII conformation and correspond well to spectra of other proline-containing peptides.[18,22]

**Manifestation of the Ring Conformation.** The ROA (and to lesser extent Raman) intensities are influenced by interactions among the proline residues. The interactions involve mechanical and electrostatic coupling and modify the internal (mono) proline signal. As they are determined by peptide length and conformation, we performed a series of trial simulations, examples of which are plotted in Figure 4 together with the experimental spectra. At the upper part of the figure, the length dependence ($Pro_n$, $n = 1, 3, 5, 10$) is simulated for equal content of both conformers (**A**,**B**). Spectra of a single proline unit (traces a, a′) were obtained by averaging eight possible triproline conformers, but polarizability tensors for atoms in the terminal residues were set to zero. Apparently, most Raman polyproline bands are present already in the spectrum of the monomer. This reflects large polarizability changes of the five-member ring coming from $CH_2$ scissoring at ~1460 $cm^{-1}$, CH wagging at ~1250 $cm^{-1}$, C−C and C−N stretching (asymmetric distortion around 1050 $cm^{-1}$, breathing mode at 930 $cm^{-1}$) and torsional (877, 540 $cm^{-1}$) ring motions. (By default, we refer to experimental wavenumbers; see more detailed mode assignments in the Supporting Information.) However, the monomer is not adequate for explanation of the ROA features, which do not stabilize until $n \geq 10$. For example, the calculated couplet signals of the ring modes (~540, 970 $cm^{-1}$) result clearly from an exciton coupling in the long helices. Although the molecular weight of the measured sample corresponds to much longer chains (~200 residues), we suppose that an effective signal corresponding to shorter helical segments ($n$ ~10) is observed due to peptide chain irregularities caused by its motion in the solution. This is consistent also with the observed Raman intensity ratio at 931 and 912 (shoulder) $cm^{-1}$, not reproducible with shorter peptide. The best agreement of simulated ROA spectra with experiment is achieved when $n \geq 10$. The longer-range correlation of vibrational motion of the proline residues explains also an overall increase of the ROA/Raman intensity ratio for longer structures.

The Raman and ROA signals are also modified by the **A**/**B** conformer proportion, varied in the middle of Figure 4 (e−g, e′−g′). Because of the coupling, a resultant signal is not a simple sum of the two conformers, not even for the vibrational modes localized at the proline ring. The 1:1 ratio provides the best overall agreement if Raman and ROA simulated intensities with experiment. Because of the limited accuracy of the simulations, however, we have to define the agreement in terms of multiple relative ROA and Raman intensities and correct ROA signs. Although most modes can be assigned reliably (average relative frequency error of 1.6%, see the Supporting Information) detailed spectral profiles are very sensitive to the mode coupling. Thus the $CH_2$ scissor signal around 1460 $cm^{-1}$ in the experimental spectra, for example, is not satisfactorily reproduced. Supposedly, our force field and the harmonic approximation do not provide correct splitting of vibrational states in this region. Also, the two-conformer model and basis set used for calculation of the ROA intensity tensors (6-31G) may not be entirely adequate. Solvent interaction should not influence significantly the simulated intensities, as the aqueous and TFE solution provided virtually the same spectral shapes. For the region around 1330 $cm^{-1}$ with a lower density of vibrational states the agreement is good for Raman, although the ROA sign pattern is modeled only roughly. The "helix mode" couplet at 1200 $cm^{-1}$ is well reproduced for the mixture while the spectrum with 100% of **B** gives a signal of opposite sign. Similarly, a 100% presence of **A** can be excluded, for example on the basis of the relative Raman intensities around 835 and 1050 $cm^{-1}$. Similarly the ROA +/− couplet 977/999 $cm^{-1}$ fits best for the **A**/**B** mixture, while for 100% of **B** the opposite sign is predicted. For another ROA couplet at 921/945 $cm^{-1}$ pure **A**, **B** conformers give the same sign, but only the mixture gives best relative intensities in the entire 900−1050 $cm^{-1}$ region. Almost no measurable ROA and a rather weak Raman signal are measured at 880−535 $cm^{-1}$ which is again consistent with the 50% traces f′,f. Below 600 $cm^{-1}$ (see the 535 $cm^{-1}$ couplet in f′ which is positively biased in experiment, the ROA signal around 400 $cm^{-1}$) the simulated ROA spectra start to deviate from the observation again. In this case, we suspect an inadequacy of the harmonic approximation, particularly the influence of the

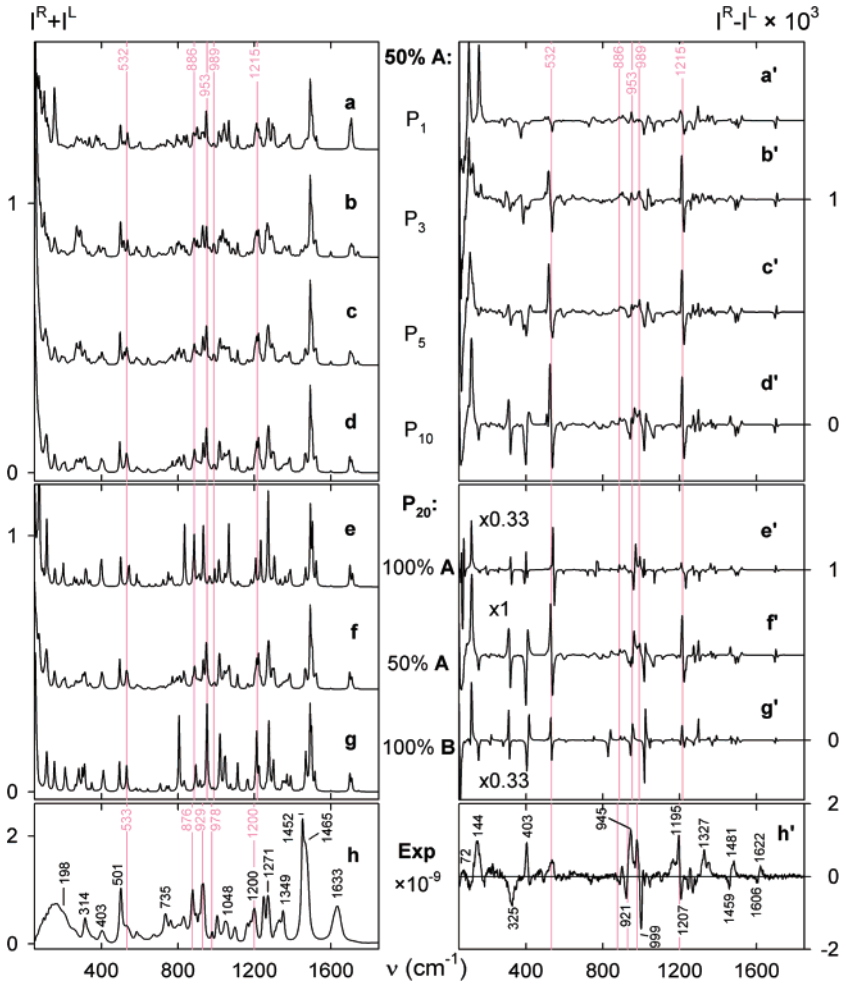


***Figure 4.*** Calculated (a−g, a′−g′) and experimental (h, h′, in aqueous solution) Raman (a−h) and ROA (a′−h′) poly-L-proline spectra. At the top, spectral dependence on the length of the polyproline chain ($P_n$, $n$ = 1, 3, 5, 10, traces a−d, a′−d′) is simulated for equal content of the two conformers. Calculated spectra of 20-proline (traces e−g, e′−g′) correspond to 100, 50, and 0% content of **A**. The red vertical lines indicate corresponding calculated and experimental bands.

proline ring dynamics (Kapitán et al., publication in preparation) that is not captured by the stationary model of the polyproline II helix. Interestingly, the Raman intensities are still reproduced very nicely in the region 200−600 cm$^{-1}$, enabling an almost band-to-band comparison with the experiment.

**Basis Set Limitations and Polarization Model.** Previous computations suggested that ab initio reproduction of ROA signs and Raman and ROA relative intensities is not extremely demanding on basis set size and ab initio level.[13,34] This is consistent with the variations of the ROA and Raman spectra modeled with the HF/6-31G, HF/6-31G, and B3LYP/6-31G** approximations in Figure 5 (all with the COSMO solvent correction and B3LYP/COSMO/6-31G** force field). The approximate polarization model[21] was used for ROA intensities so that the bigger 6-31G** basis could be consistently included. A full ROA computation at the highest B3LYP/6-31G**/COSMO level (behind the polarization model) was not possible with our means. Indeed, there are only minor differences between the HF intensities calculated with the small (6-31G, green) and bigger (6-31G**, red) bases. Bigger deviations appear between the HF and DFT computations, leading even to sign flipping of a few weak ROA bands. Interestingly, the differences are more pronounced for the lowest-energy modes. Main features, however, remain conserved, and we thus do not suppose that our analysis would be significantly hampered by the basis set incompleteness.

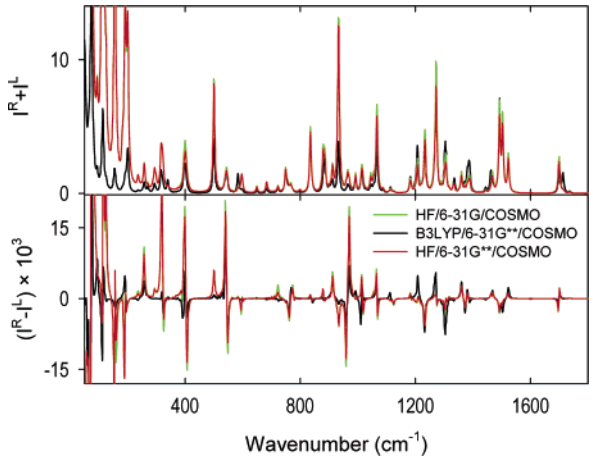


***Figure 5.*** Comparison of Raman and ROA intensities calculated at three approximation levels (HF/6-31G in green, B3LYP/6-31G** as the black line, and HF/ 6-31G* in red), all with the COSMO correction and B3LYP/COSMO/6-31G** force field. Spectra of polyproline 20-mer with 100% content of **A** were simulated; the polarization model model was used for ROA.

(34) Pecul, M.; Ruud, K. *Int. J. Quantum Chem.* **2005**, *104*, 816−829.

The polarization model provides most of the spectral features obtained also with the full simulation involving the pure magnetic and quadrupole contributions[5,29,35] (compare the HF/6-31G spectrum in Figure 5 and the corresponding trace e′ in Figure 4), although occasional sign failures for some low-intensity bands do occur. This behavior seems to be typical for polymers and larger molecules, where most of the signal is produced by a chiral orientation of multiatomic groups and chromophores.[5] On the other hand, for small molecules (alanine, unpublished results) dominated by one chiral center we observed quite a poor performance of the model. For present computations we found the model extremely useful, allowing us to quickly estimate approximate ROA profiles within a fraction of computer time needed for rigorous computations. Overall, for the case of polyproline, we can thus deduce that available computational schemes and affordable bases provide reasonable accuracy for practical purposes, despite the virtual impossibility to achieve benchmark precision for systems of this size.

**Polyproline I versus Polyproline II.** Although the ROA spectrum of the polyproline I conformation (PPI) has not been measured yet and the conformation itself can be encountered quite rarely,[36] we are naturally curious if the technique can discriminate between the two most common polyproline forms. Therefore, we performed analogous simulation of the Raman and ROA spectra for the 20-mer starting from standard polyproline I geometry.[24] For simplicity, and because our computations suggest that the **A** ring form is energetically favored in PPI, we compare the PPI and PPII spectra with the **A** side chain conformation only. According to our opinion, the difference in the Raman intensities convincingly confirms that our sample adopts the PPII conformation. The Raman bands (PPII, Figure 6), such as that at 500 $cm^{-1}$ (experimentally 501 $cm^{-1}$, see Figure 3), 749 (experimentally 734) $cm^{-1}$, and 835 (876) $cm^{-1}$ are all missing for the PPI form. For ROA (modeled within the polarization model in Figure 6) we consider important that (1) PPI and PPII provide also quite distinct spectra and (2) the intensity differences are comparable with those caused by the side-chain "perturbations".

## Conclusions

To conclude our study, we see that not only the secondary peptide structure but also side chain conformation can be indicated by ROA, although much further work is clearly needed for a more profound understanding of the spectra. Determination of the behavior of the peptide chain in full complexity may be important namely for exploration of biological processes[37] governed by relatively low-energetic changes. The extraction of the structural information requires rather sophisticated simulations which may be even more complicated for bigger or more polar residues. Although the spectral intensities relatively quickly stabilize as the peptide chain grows, consideration of the nearest neighbor coupling between proline rings is essential for the spectral interpretation. We suppose that the peptide main chain retains the polyproline II shape, as the observed spectra are consistent with other proline-containing peptides[18,22] adopting this conformation. Our analysis of the spectra indicates approximately 50(±15)% conformer populations of the two proline ring conformers in the sample.

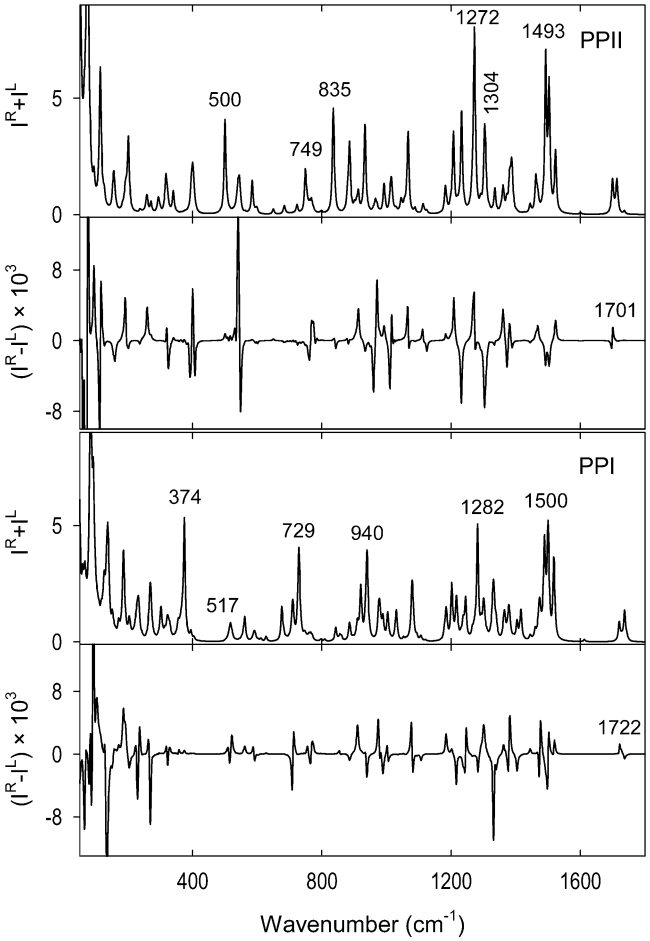


***Figure 6.*** Simulated (B3LYP/COSMO/6-31G**) Raman and ROA spectra of $(L\text{-Pro})_{20}$ in the PPI and PPII conformations. Form **A** of the proline ring was supposed; the ROA intensities are estimated within the polarizability approximation.

**Acknowledgment.** This work was supported by the Ministry of Education of the Czech Republic (MSM 0021620835).

**Supporting Information Available:** Details about ab initio geometries, spectral simulations, peak assignments, and full Gaussian reference. This material is available free of charge via the Internet at http://pubs.acs.org.

JA057337R

(35) Nafie, L. A. Raman Optical Activity. In *Modern Nonlinear Optics, Part 3*; Evans, M., Kielich, S., Eds.; Wiley: New York, 1994; Vol. 85, pp 105−206.
(36) Dukor, R. K.; Keiderling, T. A.; Gut, V. *Int. J. Pept. Protein Res.* **1991**, *38*, 198−203.
(37) Blanch, E. W.; Morozova-Roche, L. A.; Cochran, D. A. E.; Doig, A. J.; Hecht, L.; Barron, L. D. *J. Mol. Biol.* **2000**, *301*, 553−563.